

We are IntechOpen, the world's leading publisher of Open Access books Built by scientists, for scientists

6,100

Open access books available

149,000

International authors and editors

185M

Downloads

Our authors are among the

154

Countries delivered to

TOP 1%

most cited scientists

12.2%

Contributors from top 500 universities



WEB OF SCIENCE™

Selection of our books indexed in the Book Citation Index
in Web of Science™ Core Collection (BKCI)

Interested in publishing with us?
Contact book.department@intechopen.com

Numbers displayed above are based on latest data collected.
For more information visit www.intechopen.com



Chapter

N1-(3-(Trifluoromethyl)Phenyl) Isophthalamide Derivatives as Promising Inhibitors of Vascular Endothelial Growth Factor Receptor: Pharmacophore-Based Design, Docking, and MM-PBSA/MM-GBSA Binding Energy Estimation

Aliaksandr Faryna and Elena Kalinichenko

Abstract

Targeting protein kinases is a common approach for cancer treatment. In this study, a series of novel terephthalic and isophthalic derivatives were constructed as potential type 2 protein kinase inhibitors adapting pharmacophore features of approved anticancer drugs of this class. Inhibitory activity of designed structures was studied *in silico* against various cancer-related protein kinases and compared with that of known inhibitors. Obtained docking scores, MM-PBSA/MM-GBSA binding energy, and RF-Score-VS affinities suggest that N1-(3-(trifluoromethyl) phenyl) isophthalamide could be considered as promising scaffold for the development of novel protein kinase inhibitors which are able to target the inactive conformation of vascular endothelial growth factor receptor.

Keywords: terephthalic and isophthalic derivatives, anticancer activity, VEGFR, virtual screening, MM-PBSA/MM-GBSA, docking

1. Introduction

Since its approval in 2001, imatinib has revolutionized drug therapy of chronic myeloid leukemia (CML) [1, 2]. Imatinib is a selective inhibitor of a specific protein – BCR-ABL tyrosine kinase, which biosynthesis is encoded by the Philadelphia chromosome, which is characteristic for all CML cells [3, 4]. High and uncontrolled activity of this protein leads to disruption of cell signaling causing a rapid growth of

the tumor tissue. Imatinib has secured more than 80% 8-year overall survival rate in patients with CML, almost double compared to the previous drugs generation [5, 6].

The clinical success of imatinib has fueled an explosion in the protein kinase inhibitor research. The strategy of blocking signaling pathways mediated by an overexpression or deregulation of certain protein kinases has proven to be effective in treating many other cancers as well as some non-cancer diseases. More than seventy drugs of this class have now been registered, targeting dozens of various kinase targets, which constitutes about 10% of the total number of kinases encoded by the human genome [7, 8]. Besides BCR-ABL, another large group of drugs targets various growth factors receptors (epidermal, platelet, vascular endothelial, etc.) [9, 10].

The use of protein kinase inhibitors for cancer treatment has some limitations. First of all, an important problem is drug resistance in patients. Resistance can occur initially (primary resistance) or over time (secondary resistance) [11–13]. One of the key mechanisms of secondary resistance is the emergence of the mutants of the primary target, which appears with the disease progression. Binding affinity of an inhibitor to the mutant target is significantly lower. In some cases, such mutations completely block binding [14–19].

The second key consideration is inhibitor selectivity. Since all protein kinases accept ATP as a substrate, there is a high structural similarity between the active sites of different protein kinases. An inhibitor usually does not act exclusively on its main target but can suppress, to some degree, the activity of some or many other kinase targets. So, such multitargetness can be a positive (e.g. when cancer cells express several types of kinases) or a negative factor – side inhibition can be the cause of adverse effects [20, 21]. Selectivity modulation becomes even more problematic with the disease progression as it is accompanied by further genetic degradation of cancer cells [22, 23]. For example, in the case of CML, the optimal choice for a second-line therapy inhibitor between dasatinib, bosutinib, and nilotinib can be made based on a personalized assessment of the actual kinase overexpression profile [24].

Since the efficacy of treatment with protein kinase inhibitors depends significantly on the time of treatment initiation, the most important property of a drug is its actual inhibitory activity, including that toward mutant targets. For example, nilotinib, a second-generation structural analog of imatinib, has been initially considered as a second-line therapy option [25]. Further investigations have showed that this drug could be more effective than imatinib as a first-line therapy being a more potent inhibitor of BCR-ABL and its mutants [26, 27].

Therefore, the search for the novel highly effective inhibitors of therapeutically relevant protein kinases with a given selectivity and the ability to suppress mutant targets is still an important scientific challenge.

In this context, the recent advances in the development of molecular modeling techniques for the search of biologically active compounds cannot be overlooked. The literature describes cases of successful application of pharmacophore screening [28, 29], molecular docking, and molecular dynamics [30–32] to identify new chemical structures with anti-kinase activity. In addition, the improvements in technical and theoretical background of machine learning algorithms have made it possible to adapt them, *inter alia*, for the modeling of protein-ligand interactions [33–36].

The present work continues our previous studies on the design of novel potential protein kinase inhibitors using directed pharmacophore design and molecular modeling [37, 38]. In this case, the object of such studies is new derivatives of terephthalic and isophthalic acids, which are designed in a manner to give the structures significant pharmacophore similarity to known type 2 protein kinase inhibitors.

The potential anti-kinase activity of the designed terephthalic and isophthalic acids derivatives has been investigated by molecular docking, molecular dynamics, as well as by using machine learning model for virtual screening RF-Score-VS [39].

2. Materials and methods

2.1 Design of target structures

X-ray diffraction data have revealed a number of common patterns in terms of binding of known protein kinase inhibitors to their targets. Two large groups of inhibitors can be distinguished. Type 1 inhibitors are direct ATP competitors and bind to the active center of the biologically active conformation of a protein kinase. Most of the approved inhibitors are type 1 inhibitors. However, in the case of imatinib, the binding is of a slightly different nature. The loop that links the two main lobes of BCR-ABL tyrosine kinase is flexible and in a certain position opens up an additional allosteric pocket adjacent immediately to the ATP binding site, thus extending the active center of the enzyme [40]. At the same time, the structure of the ATP pocket changes significantly, so it is unable to accept the natural substrate. Such inactive conformations can be seen for many others protein kinases. Inhibitors that bind to this inactive conformation of a protein kinase target are classified as type 2 inhibitors [41]. The described classification to this most common inhibitor classes is not perfectly strict, since there are stable intermediate kinase conformations with different volumes of allosteric pocket available and it is hard to classify ligand binding as type 1 or type 2 unambiguously [42].

In the structure of type 2 inhibitors, a number of key structural and pharmacophore features can be distinguished. Firstly, there is a benzamide fragment, most often with the 3-trifluoromethyl substituent in the benzene ring, which facilitates the formation of the necessary interactions, including hydrogen bonds, in the allosteric pocket of the active center. Secondly, the structure of type 2 inhibitors contains a heteroaromatic system, which in some sense imitates adenine but can form hydrogen bonds in the modified ATP pocket, which has been subjected to the structural changes upon the transition of a kinase to the inactive conformation. The relative orientation of these structural fragments is managed by the linker, which is usually represented by a benzene ring containing substituents in different positions [43–46].

In our previous studies, we have used the 4-methylbenzamide linker as a framework for constructing novel type 2 protein kinase inhibitors and that are allowed us to identify novel bioactive compounds with actual inhibitory activity against protein kinases [37, 38].

In this study, we have proposed that isophthalic and terephthalic acids transform into appropriate amides as a promising linkers for developing potential protein kinase inhibitors (**Figure 1**). In our opinion, the use of such linkers may be favorable for several reasons. For instance, these structures contain an amide bond, which is necessary for the formation of hydrogen bonds in the allosteric pocket of a kinase binding pocket. In addition, the overall size of linkers corresponds to those in the structures of known inhibitors. Moreover, the presence of a second carboxylic group may lead to the formation of hydrogen bonds in the ATP pocket. If compared to 4-methylbenzamide this linkers are more rigid, which may have a positive effect on kinase binding affinity. It is also important to note that we have used both isophthalic and terephthalic fragments to more fully study the conformational space of the linker

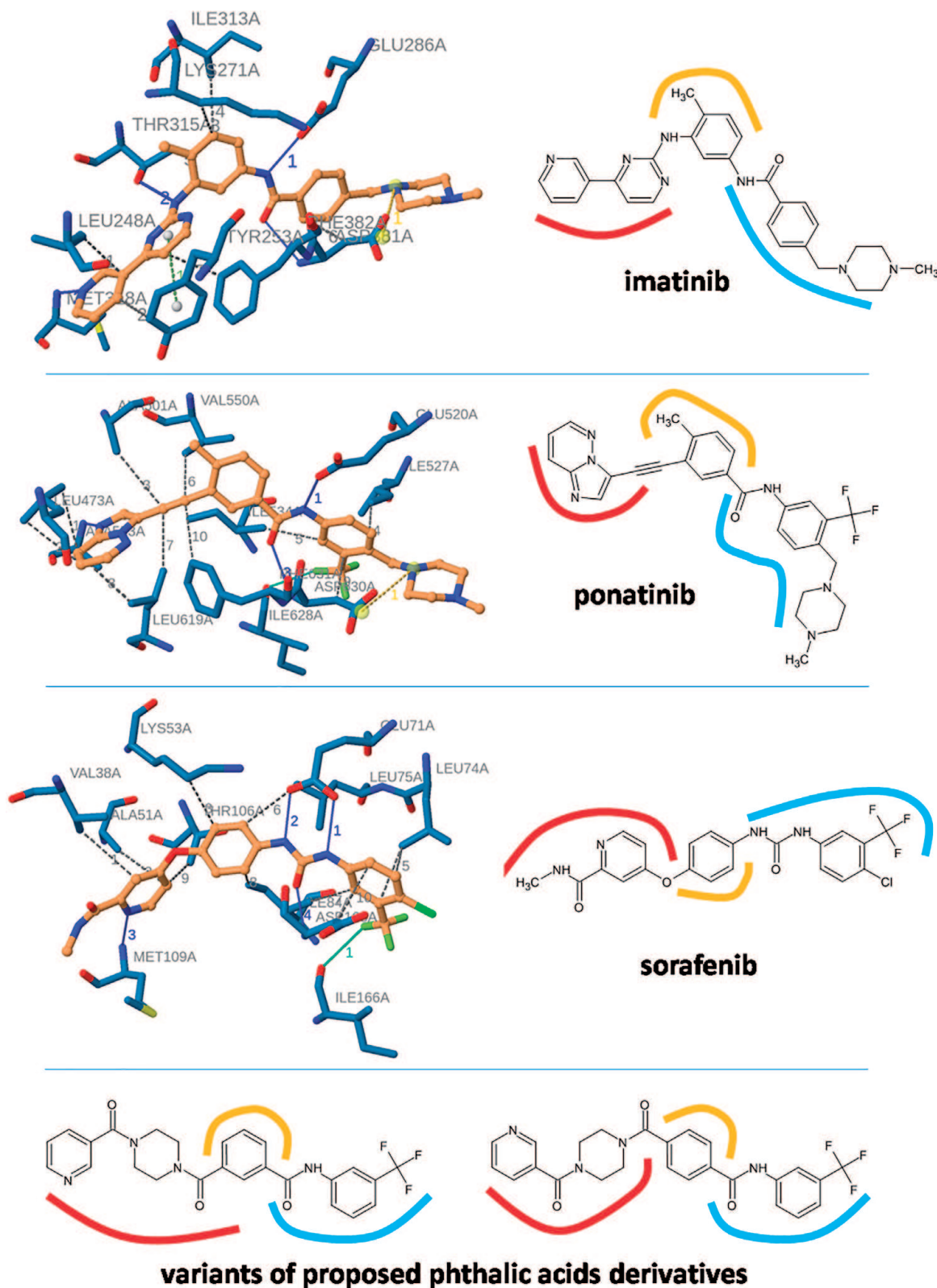


Figure 1. Pharmacophore features of approved type 2 protein kinase inhibitors and proposed structures. Structural fragments that bind to different regions of binding site are highlighted with red (ATP pocket), blue (allosteric pocket), and orange (linker). Interactions were obtained by PLIP [47].

region. By varying the mutual arrangement of carbonyl groups, it could be possible to determine which linker is more suitable to be placed in a kinase's binding site.

On the basis of selected linkers, we have generated a library of novel chemical structures by introducing different amines into the carbonyl groups of phthalic acids

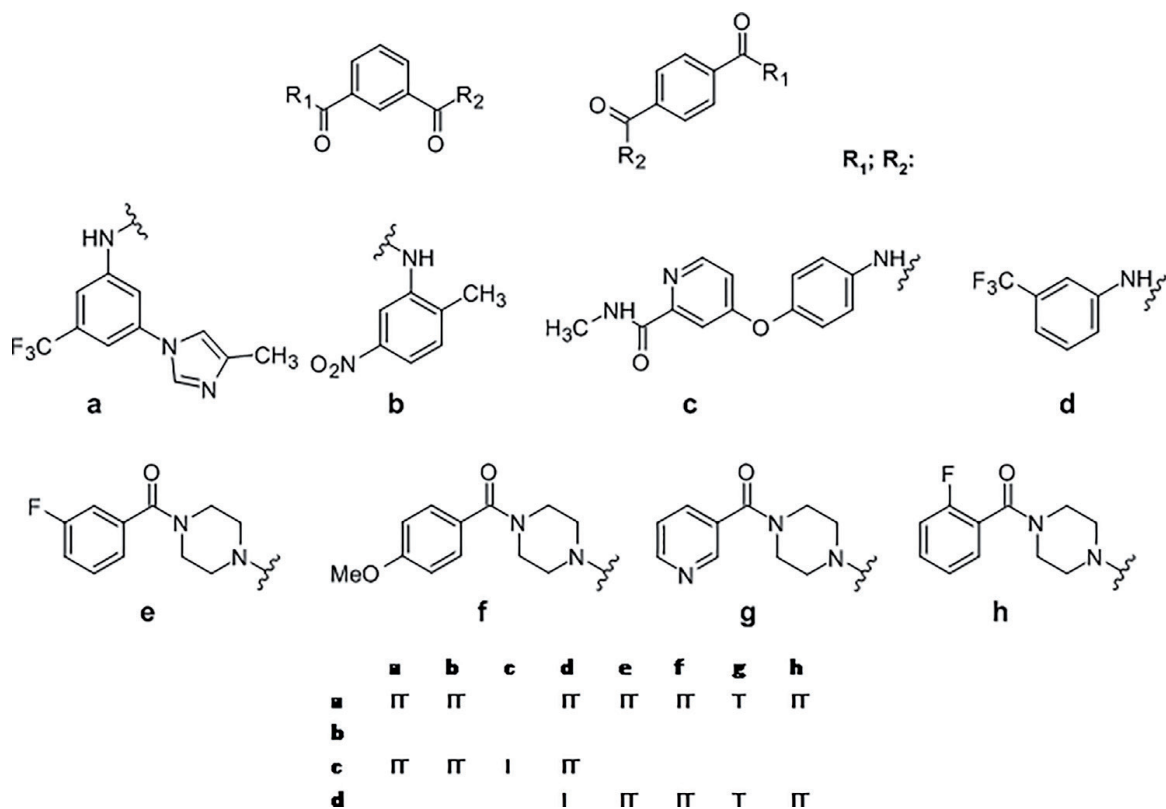


Figure 2. The generation scheme of studied phthalic acids derivatives. Letters a–h represent amine substituents. Letters I, T, and IT represent what type of linker was used for a structure: Isophthalic, terephthalic, or both.

to study their potential anti-kinase activity by molecular modeling and molecular docking. A total of 28 unique chemical structures are generated (**Figure 2**). As substituents at carbonyl groups of phthalic linkers, we have used structural fragments of known inhibitors: 3-trifluoroaniline (nilotinib, ponatinib, and sorafenib), 4-(4-aminophenoxy)-N-methylpyridine-2-carboxamide (sorafenib), and other amines convenient in terms of commercial availability and possibility of further derivatization.

2.2 Docking

For molecular docking experiments, 3D structures of studied phthalic acid derivatives are generated using the Cactus service [48]. For docking studies, we have used open-source software AutoDock Vina [49] as Qvina 2.1 [50] modification.

The 3D structures of 33 cancer-relevant protein kinases are used as docking receptors. Their structures are obtained from the database of experimental X-ray data The Protein Data Bank (PDB) [51]. Most of the receptors are protein kinases of different families. Two receptors are poly (ADP-ribose)-polymerases as this protein class is also used for targeted cancer therapy [52] (**Table 1**).

Docking of the constructed ligands and receptors is performed using “each to each” scheme. Coordinates of active centers for Qvina are generated based on a visual assessment of the location of native ligands from PDB complexes with an increase of approximately 10–30% in each dimension. The Qvina search exhaustiveness parameter is set to 24. The preparation of receptors and ligands for the docking has been performed using Chimera 1.13.1 [54].

	PDB code	Protein family	Original (native) ligand	Ligand binding type
1	1r0p	c-Met	Alkaloid K-252a	1
2	2bfy	Aurora-B	Hesperadin	1
3	2hyy	Abl	Imatinib	2
4	2in6	Wee1	PD311839	1/2
5	2pl0	Lck	Imatinib	2
6	2vrz	Aurora-B	ZM447439	1/2
7	3bbt	ErbB4 (Her4)	Lapatinib	1/2
8	3cs9	Abl	Nilotinib	2
9	3gcs	P38-Map	Sorafenib	2
10	3hng	Vegfr1	N-(4-chlorophenyl)-2-[(pyridin-4-ylmethyl)amino]benzamide	2
11	3og7	Braf V600E	PLX4032	2
12	3pp0	ErbB2 (Her2)	2-{2-[4-({5-chloro-6-[3-(trifluoromethyl)phenoxy]pyridin-3-yl)amino]-5H-pyrrolo[3,2-d]pyrimidin-5-yl]ethoxy}ethanol	2
13	3qrj	Abl T315I	Rebastinib (DCC-2036)	2
14	3wze	Vegfr2 (kdr)	Sorafenib	2
15	3zbf	Ros1	Crizotinib	1
16	4ag8	Vegfr2	Axitinib (AG-013736)	2
17	4asd	Vegfr2	Sorafenib	2
18	4at3	Trkb	CPD5N	1/2
19	4b8m	Aurora-B	VX-680	1/2
20	4c2w	Aurora-B	ATP	1
21	4dce	Alk	(3S)-N-(4-methylbenzyl)-1-{2-[(3,4,5-trimethoxyphenyl)amino]pyrimidin-4-yl}piperidine-3-carboxamide	1/2
22	4g5p	Egfr T790M	BIBW2992	1
23	4lmn	Mek1	GDC0973 + ATP	—
24	4tvj*	Parp2	Olaparib	—
25	5ew9	Aurora A	MK-5108	1
26	5hi2	Braf	Sorafenib	2
27	5kup	Btk	6-{tert}-butyl-8-fluoranil-2-[3-(hydroxymethyl)-4-[1-methyl-6-oxidanylidene-5-(pyrimidin-4-ylamino)pyridin-3-yl]pyridin-2-yl]phthalazine-1-one	
28	5kvt	Trka	Entrectinib	1
29	5toz**	Jak3	PF-06651600	1
30	5y5u	Syk	4-[(1-methylindazol-5-yl)amino]-2-(4-oxidanylpiperidin-1-yl)-8H-pyrido[4,3-d]pyrimidin-5-one	1

31	6kzd	Trkc	3-[2-[6-(4-aminofenyl)imidazo[1,2-a]pyrazin-3-yl]ethynyl]-2-methyl-[N]-[3-(4-methylpiperazin-1-yl)-5-propan-2-yl-phenyl]benzamide	2
32	6nec	Ret	Nintedanib	1
33	7kk4*	Parp1	Olaparib	—

**A receptor is poly (ADP-ribose)-polymerase.*
***A ligand is a covalent inhibitor – it binds to the receptor by forming a chemical bond [53].*

Table 1.
 Receptors used for the docking studies.

2.3 Molecular dynamics

After the docking step, the most promising protein-ligand complexes have been subjected to molecular dynamics simulation for more accurate binding affinity estimation. The complexes for the simulation are selected based on the obtained docking scores. The open-source GROMACS 2019.1 [55] software is used to conduct molecular dynamics experiments. The standard molecular dynamics protocol includes a minimization step, two 200 ps equilibration steps, and a final 2 ns simulation. The resulting molecular dynamics trajectory is used to estimate the binding energy, which is performed in three ways. All ligands are parameterized by Acypype [56]. Complete md-protocol is described in previous work [37].

The first two calculation methods include the implementations of the molecular mechanics Poisson-Boltzmann surface area (MM-PBSA) and molecular mechanics-generalized Born surface area (MM-GBSA) [57]. These methods are widely used to estimate inhibitory activity for protein-ligand complexes. Their main advantage is the relatively high accuracy of obtained results along with a simpler system setup procedure if compared to the thermodynamic integration or free energy perturbation methods [58]. A relatively short simulation time is chosen based on the published evidence that the accuracy of the MM-PBSA/MM-GBSA protocols is in many cases independent of simulation time, and in some experiments a short simulation time is preferable [59].

In our case, the MM-PBSA/MM-GBSA binding energy calculation has been carried out using two kinds of softwares: `g_mmpbsa` [60] and `gmx_MMPBSA` [61]. The main difference between these programs, apart from the technical implementation, is that `g_mmpbsa` only calculates the Poisson-Boltzmann surface area (PBSA) variant, whereas `gmx_MMPBSA` allows to also using the generalized Born surface area (GBSA) and also provides entropy change estimation.

The third approach used provides the estimation of the binding affinity of the studied phthalic derivatives applying the RF-Score-VS (Random Forest-based scoring function for Virtual Screening) machine learning algorithm [39]. This algorithm uses a “set of decision trees” model trained on a large set of active and inactive docking poses. The main purpose of RF-Score-VS is to refine the estimation of docking results. In training procedure for this model, a set of deliberately inactive ligands are used aimed to increase the probability of distinguish real “hits” between the structures with the highest scores. This is what makes RF-Score-VS different from many other rescoring protocols, including RF-Score v3 [62] from the same authors, which are focused on more accurate numerical estimation of binding energy for known ligands. According to the published data [39], the RF-Score-VS model is significantly superior

to the AutoDock Vina scoring function in terms of the probability of finding a real inhibitor. In our study, we have extended the scope of RF-Score-VS uses by applying it not to the obtained docking pose, but to the frames of the resulting molecular dynamics trajectory. In our opinion, this approach can be more accurate as it takes into account time-dependent changes of the protein-ligand complex reflected by the simulation. At the same time, the computing expenses remain acceptable.

In all three methods, we did not use the full 2-ns-long trajectory of the complex, but every 20th frame skipping first 200 ps of the production run.

3. Results and discussion

After docking stage, we obtained 924 complexes of the studied structures along with the corresponding docking scores representing binding energy estimation. In order to study any binding patterns, the resulting docking poses were filtered based on their binding energy. Docking scores better or equal to -11.5 kcal/mol were used as a threshold for filtering. This threshold was chosen based on our previous experience. After filtering, we obtained 133 docking poses out of 924 that showed such a high binding energy. We investigated then the distribution of filtered docking poses by linker type (isophthalic or terephthalic), by the most frequent amine fragments and by receptor type.

Out of 133 poses with high docking scores, 101 poses corresponded to the structures containing an isophthalic linker; therefore, 22 poses belonged to the structures having terephthalic linker. This ratio remained virtually unchanged when the filtration threshold was increased: 63/12 for the threshold of 12.0 kcal/mol and better, 30/8 at 12.5 kcal/mol, and 20/5 at 13.0 kcal/mol.

The distribution of amine substituents in high-scoring docking poses is shown in **Figure 3**. Amines containing 3-trifluoromethylaniline are the most frequent.

The most frequent receptors in protein-ligand complexes with a score of -11.5 kcal/mol and better are trkc kinase (PDB: 6kzd), abl family (PDB: 3cs9, 2hyy), and vegfr family (PDB: 3hng, 3wze, 4asd), as shown in **Figure 4**. It is important to note that all of these receptors are essentially protein kinases being in inactive conformation accepting type 2 ligands, which indirectly confirms the correctness of the chosen approach to the design of studied phthalic derivatives.

The obtained docking results indicate that the isophthalic linker, together with the attached 3-trifluoromethylaniline, might be a promising structural fragment in terms of its ability to bind to protein kinases as type 2 inhibitor.

At the second stage, we selected 25 complexes of the studied structures that were obtained during the docking step to refine ligand binding energies using molecular dynamics methods. The complexes for molecular dynamics simulation were chosen based on their docking score and to get a certain degree of diversity in chosen linkers and receptors. Out of 25 complexes, seven had terephthalic linker and 18 contained isophthalic linker.

After conducting a 2-ns simulation for each complex, we calculated the binding energy via processing the obtained trajectory frames using three methods: MM-PBSA (g_mmpbsa), MM-GBSA (gmx_mmpbsa), and rescoring with the RF-Score-VS scoring function. The last is based on a machine learning model (**Table 2**).

It was of particular interest for us to compare the results obtained by three methods of binding energy estimation. In our case, the values of electrostatic and van der Waals interactions obtained by g_mmpbsa (MM-PBSA) and gmx_mmpbsa

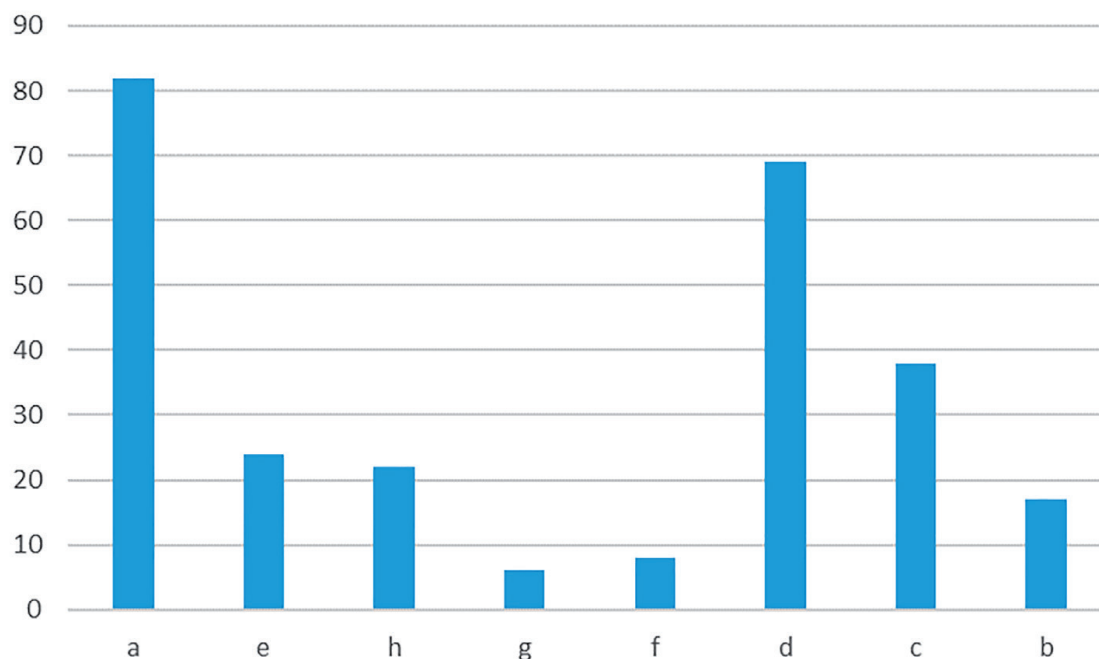


Figure 3.
Frequency of different amine fragments appearing in docking poses with a score of -11.5 kcal/Mol and better.

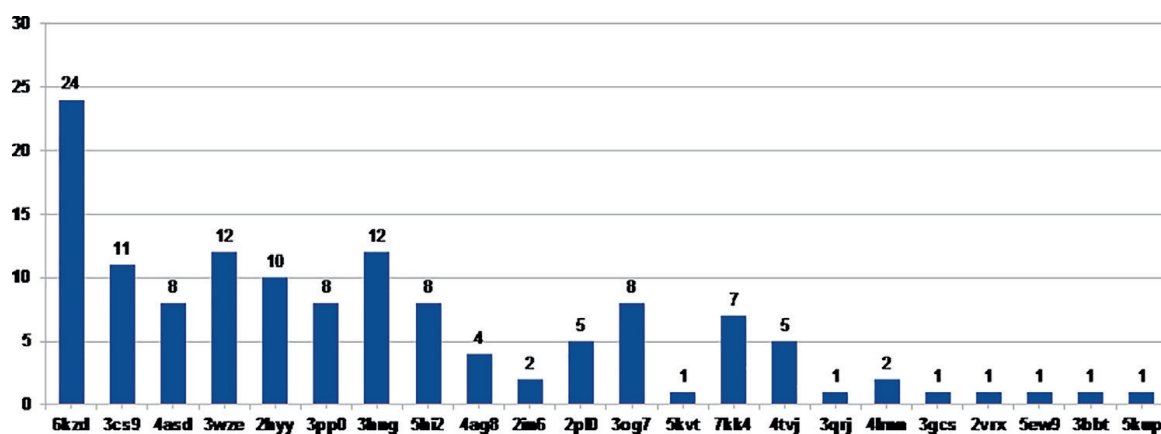


Figure 4.
Distribution of docking poses with a score of -11.5 kcal/Mol and better by receptor type.

(MM-GBSA) are in strict linear correlation with each other (**Figure 5**), which indicates that the methods for calculating the molecular-mechanical component of binding energy in these two tools are uniform.

When taking into account the solvation component, the correlation between these two methods decreases but remains high with the correlation coefficient $R^2 = 0.76$. The decrease in correlation can be naturally explained by the differences in the estimation of the solvation component of binding energy applying the Poisson-Boltzmann surface area and the generalized Born surface area. When the entropic component of gmx_mmpbsa is added, the correlation coefficient decreases slightly more but remains high ($R^2 = 0.66$). Thus, in general, both used programs show similar results for the same complexes.

We also compared the results obtained from MM-PBSA/MM-GBSA calculations with those of RF-Score-VS machine learning algorithm. The RF-Score-VS values moderately correlated both with the g_mmpbsa ($R^2 = 0.50$) and gmx_mmpbsa ($R^2 = 0.51$)

pdb	Linker	Amines		gmx_mmpbsa, kcal/mol				RF-score	g_mmpbsa, kJ/mol		
				v.d.w.	electr.	entr.	total		v.d.w.	electr.	total
3wze	iso	c	a	-71,1	-26,2	9,9	-48,8	6,5	-297,4	-54,7	-150,5
6kzd	iso	a	f	-65,8	-40,7	17,8	-31,4	6,3	-275,3	-85,14	-95,59
6kzd	iso	a	h	-62,7	-4,4	16,2	-31,4	6,1	-262,3	-9205	-111,5
3cs9	iso	a	h	-72,6	-13,5	6	-53,3	6,3	-303,5	-28,01	-144,9
6kzd	iso	a	e	-70,1	-20	9,9	-45,6	6,2	-293,4	-41,89	-137,9
6kzd	tere	a	h	-69,6	-19	18,7	-38,8	6,2	-291,3	-39,37	-141,1
6kzd	iso	d	h	-59,3	-2,4	13,3	-34,5	6,0	-248	-5111	-123,5
6kzd	tere	d	e	-58,1	-29,8	8,6	-39,3	6,0	-243,1	-62,39	-128,4
6kzd	iso	d	e	-48,5	-30,7	14,4	-21,5	6,0	-202,8	-64,39	-76,8
3 pp0	iso	d	e	-55,6	-9,1	7,7	-34,1	6,0	-232,6	-19,04	-96,72
6kzd	tere	a	e	-63,8	-5,5	15,2	-27,4	6,2	-266,7	-11,69	-125,9
5hi2	iso	d	h	-57,4	-27,4	7	-46,6	6,1	-240,2	-57,45	-118,9
3cs9	iso	d	h	-62,6	-14	13,2	-41	6,2	-262	-29,21	-128,6
3wze	iso	a	h	-74	-30,8	7,4	-64	6,5	-309,6	-64,57	-157
3wze	tere	d	e	-51,9	-30,3	8	-34,7	6,0	-217	-63,19	-85,65
6kzd	tere	a	g	-69,2	-12,5	9,9	-40,8	6,4	-289,5	-26,05	-134,3
3cs9	iso	c	a	-77,1	-37,1	9,1	-47,9	6,3	-322,3	-77,15	-144,4
3cs9	iso	d	f	-68	-21,6	13,8	-46	6,1	-284,4	-43,96	-141,8
6kzd	tere	a	f	-69,8	-22,4	14,2	-37	6,2	-291,8	-46,92	-149
4asd	iso	c	a	-79,9	-33,8	10,1	-53,6	6,5	-334,2	-70,75	-155,3
3hng	iso	a	d	-64,9	-22,6	16	-36,8	6,3	-271,3	-47,31	-119,6
3 pp0	tere	d	h	-50,8	-15,6	11,5	-26,7	6,0	-212,6	-32,59	-86,55

4ag8	iso	c	a	-76,4	-34,4	9,3	-53,5	6,5	-319,5	-71,87	-150,8
4ag8	iso	a	d	-65,4	-23,2	11,2	-44	6,2	-273,6	-49,12	-138,8
4ag8	iso	d	f	-65,2	-33,1	7,7	-58	6,2	-272,9	-69,09	-148,4
Reference ligands											
2hyy	imatinib			-67,4	-20,1	5,3	-50,5	6,2	-282,1	-42,4	-154,7
3cs9	nilotinib			-72,8	-28,1	6,1	-56,1	6,6	-304,6	-57,8	-183,1
3 pp0	original			-71	-19,5	12,7	-50,2	6,5	-297,1	-41,1	-143,6
6kzd	original			-82,6	-37,7	8,2	-61	6,4	-345,5	-66,2	-206,9

Table 2.
Calculated binding affinities of studied and reference structures to their receptors.

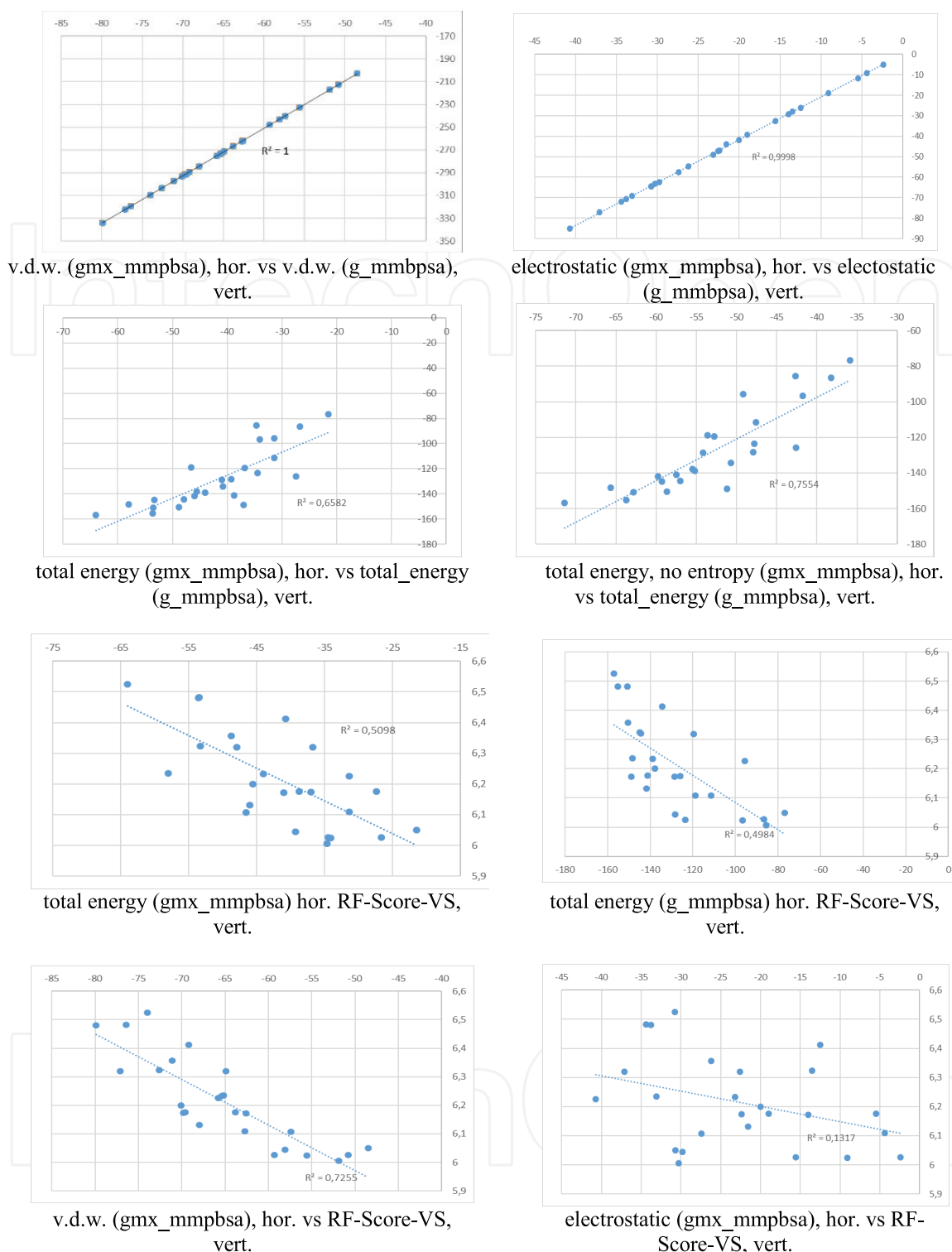


Figure 5. Correlations between binding affinities obtained by different approaches.

final scores. It is noteworthy that the correlation between RF-Score-VS values and the van der Waals component of MM-PBSA/MM-GBSA binding energy is quite high ($R^2 = 0.73$) and extremely low for the electrostatic component ($R^2 = 0.13$).

All used methods for binding energy estimation are known to be more efficient for the relative ranking of potential inhibitors than for the precise calculation of absolute binding energy. Therefore, we have used known inhibitors as reference structures. In most cases, the studied phthalic derivatives showed worse binding energy scores

compared to known inhibitors. The latter, in turn, were characterized by relatively high binding energy scores regardless the applied method for the calculation. Among the known inhibitors, the highest RF-Score-VS scores were observed for nilotinib (PDB id: 3cs9). Extremely high MM-PBSA/MM-GBSA energies were obtained for the native ligand of trkc kinase complex (PDB id: 6kzd). In the case of abl-protein kinase, nilotinib, being a second-generation inhibitor, showed higher estimated activity compared to the first-generation drug imatinib.

Among the studied phthalic acid derivatives, two structures can be distinguished which showed high binding energy scores calculated by all three methods. Both of these structures are isophthalic acid derivatives and contain a 5-imidazolyl-3-trifluorophenyl fragment of nilotinib. The second carboxyl group in these structures is modified by 4-(4-aminophenoxy)-N-methylpiperazine (sorafenib fragment) and (2-fluorophenyl) (piperidin-1-yl) methanone **h**, respectively. If compared to known inhibitors, high *in silico* inhibitory activity of these structures was observed for vegfr receptors (pdb ids: 4asd, 4ag8, 3wze) and, to a slightly lesser extent, for abl (3cs9).

Several complexes of two aforementioned structures have been subjected to hydrogen bonds analysis. For the frames of the molecular dynamics trajectory, hydrogen bonds are searched using GROMACS hbond module. The frames with the highest number of hydrogen bonds have been visualized. Visualization shows that these structures bind to the active center similar to known type 2 inhibitors: the 3-trifluoromethylaniline fragment occupies the allosteric pocket and the isophthalic acid fragment plays a linker role. In both cases, the allosteric amide bond forms two hydrogen bonds with amino acid residues of asparagine and glutamine, which is typical for type 2 inhibitors. (**Figure 6**). Regarding the ATP binding site, our analysis shows that the carbonyl group of phenyl (piperazin-1-yl) methanone may be involved in hydrogen bonding. In the case when 4-(4-aminophenoxy)-N-methylpiperazine is located in this region, hydrogen bonds can be formed by oxygen atoms of phenolic and carbonyl groups. Hydrogen bonds of the non-allosteric amide bond of the phthalic linker have not been detected.

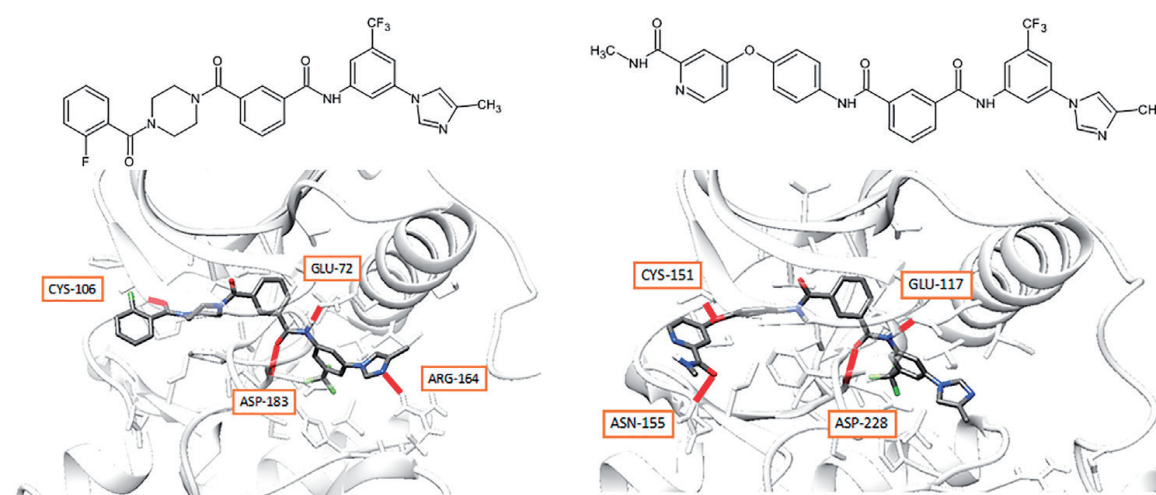


Figure 6. Structure of most promising structures and the visualization of their binding to receptors. The binding of 3-(4-(2-fluorobenzoyl)piperazine-1-carbonyl)-N-(3-(4-methyl-1H-imidazol-1-yl)-5-(trifluoromethyl)phenyl)benzamide to vegfr is shown on the left (PDB id: 3wze, h-bonds: Cys-106, Asp-183, Glu-72, Arg-164). The binding of N1-(3-(4-methyl-1H-imidazol-1-yl)-5-(trifluoromethyl)phenyl)-N3-(4-((2-(methylcarbamoyl)pyridin-4-yl)oxy)phenyl)isophthalamide to vegfr is shown on the right (PDB id: 4asd, h-bonds: Cys-151, Asn-155, Asp-228, Glu-117).

4. Conclusions

In this study, 28 unique chemical structures of new derivatives of terephthalic and isophthalic acids have been studied. These structures are designed in such a way as to give the structures a significant pharmacophore similarity with known type 2 protein kinase inhibitors. Three-dimensional structures of 33 protein kinases associated with cancer have been used as docking receptors. At the same time, most of the receptors represent protein kinases of different families. The obtained docking parameters, the binding energy of MM-PBSA/MM-GBSA, and the affinity of RF-Score-VS suggest that the isophthalic linker together with the attached 3-trifluoromethylaniline may be a promising structural fragment in terms of its ability to bind to protein kinases as a type 2 inhibitor. In comparison with known inhibitors, high inhibitory activity of isophthalic structures in silico are observed for vegfr (pdb ids: 4asd, 4ag8, 3wze) receptors and to a somewhat lesser extent for abl (3cs9). If compared to known inhibitors, high in silico inhibitory activity of these structures was observed for vegfr receptors (pdb ids: 4asd, 4ag8, 3wze) and, to a slightly lesser extent, for abl (3cs9). At the same time, the use of terephthalic acid for this purpose is ineffective. The most promising structural fragment is 1-[3-(trifluoromethyl)phenyl]benzene-1,4-dicarboxamide. By introducing different substituents to the free amino group to this structure, the anti-kinase activity of the obtained chemical compounds can be expected.

Acknowledgements


This research was funded by the National Academy of Sciences of Belarus within the research project number 2.3.2.1 of State Program for Scientific Research “Chemical basis of life processes (bioorganic chemistry).”

Author details

Aliaksandr Faryna* and Elena Kalinichenko
Institute of Bioorganic Chemistry, National Academy of Sciences of Belarus, Minsk, Belarus

*Address all correspondence to: farina@iboch.by

IntechOpen

© 2022 The Author(s). Licensee IntechOpen. This chapter is distributed under the terms of the Creative Commons Attribution License (<http://creativecommons.org/licenses/by/3.0>), which permits unrestricted use, distribution, and reproduction in any medium, provided the original work is properly cited. 

References

- [1] Kantarjian HM, Talpaz M. Imatinib mesylate: Clinical results in Philadelphia chromosome-positive leukemias. *Seminars in Oncology*. 2001;**28**(5 Suppl. 17):9-18
- [2] Lyseng-Williamson K, Jarvis B. Imatinib. *Drugs*. 2001;**61**(12):1765-1776. DOI: 10.2165/00003495-200161120-00007
- [3] Druker BJ, Tamura S, Buchdunger E, et al. Effects of a selective inhibitor of the Abl tyrosine kinase on the growth of Bcr-Abl positive cells. *Nature Medicine*. 1996;**2**(5):561-566. DOI: 10.1038/nm0596-561
- [4] Witte ON, Dasgupta A, Baltimore D. Abelson murine leukaemia virus protein is phosphorylated in vitro to form phosphotyrosine. *Nature*. 1980;**283**(5750):826-831. DOI: 10.1038/283826a0
- [5] Kantarjian H, O'Brien S, Jabbour E, et al. Improved survival in chronic myeloid leukemia since the introduction of imatinib therapy: A single-institution historical experience. *Blood*. 2012;**119**(9):1981-1987. DOI: 10.1182/blood-2011-08-358135
- [6] Hochhaus A, Larson RA, Guilhot F, et al. Long-term outcomes of Imatinib treatment for chronic myeloid leukemia. *The New England Journal of Medicine*. 2017;**376**(10):917-927. DOI: 10.1056/NEJMoa1609324
- [7] Roskoski R Jr. Properties of FDA-approved small molecule protein kinase inhibitors: A 2022 update. *Pharmacological Research*. 2022;**175**:106037. DOI: 10.1016/j.phrs.2021.106037
- [8] Cohen P, Cross D, Jänne PA. Kinase drug discovery 20 years after imatinib: Progress and future directions. *Nature Reviews. Drug Discovery*. 2021;**20**(7):551-569. DOI: 10.1038/s41573-021-00195-4
- [9] Ghosh S, Marrocco I, Yarden Y. Roles for receptor tyrosine kinases in tumor progression and implications for cancer treatment. *Advances in Cancer Research*. 2020;**147**:1-57. DOI: 10.1016/bs.acr.2020.04.002
- [10] Kleczko EK, Heasley LE. Mechanisms of rapid cancer cell reprogramming initiated by targeted receptor tyrosine kinase inhibitors and inherent therapeutic vulnerabilities. *Molecular Cancer*. 2018;**17**(1):60. DOI: 10.1186/s12943-018-0816-y
- [11] Lovly CM, Shaw AT. Molecular pathways: Resistance to kinase inhibitors and implications for therapeutic strategies. *Clinical Cancer Research*. 2014;**20**(9):2249-2256. DOI: 10.1158/1078-0432.CCR-13-1610
- [12] Tartarone A, Lazzari C, Lerosé R, et al. Mechanisms of resistance to EGFR tyrosine kinase inhibitors gefitinib/erlotinib and to ALK inhibitor crizotinib. *Lung Cancer*. 2013;**81**(3):328-336. DOI: 10.1016/j.lungcan.2013.05.020
- [13] Lamontanara AJ, Gencer EB, Kuzyk O, Hantschel O. Mechanisms of resistance to BCR-ABL and other kinase inhibitors. *Biochimica et Biophysica Acta*. 2013;**1834**(7):1449-1459. DOI: 10.1016/j.bbapap.2012.12.009
- [14] Dong RF, Zhu ML, Liu MM, et al. EGFR mutation mediates resistance to EGFR tyrosine kinase inhibitors in NSCLC: From molecular mechanisms to clinical research. *Pharmacological Research*. 2021;**167**:105583. DOI: 10.1016/j.phrs.2021.105583

- [15] Daver N, Schlenk RF, Russell NH, Levis MJ. Targeting FLT3 mutations in AML: Review of current knowledge and evidence. *Leukemia*. 2019;**33**(2):299-312. DOI: 10.1038/s41375-018-0357-9
- [16] Yu HA, Arcila ME, Hellmann MD, Kris MG, Ladanyi M, Riely GJ. Poor response to erlotinib in patients with tumors containing baseline EGFR T790M mutations found by routine clinical molecular testing. *Annals of Oncology*. 2014;**25**(2):423-428. DOI: 10.1093/annonc/mdt573
- [17] Castellanos E, Feld E, Horn L. Driven by mutations: The predictive value of mutation subtype in EGFR-mutated non-small cell lung cancer. *Journal of Thoracic Oncology*. 2017;**12**(4):612-623. DOI: 10.1016/j.jtho.2016.12.014
- [18] Roskoski R Jr. Targeting oncogenic Raf protein-serine/threonine kinases in human cancers. *Pharmacological Research*. 2018;**135**:239-258. DOI: 10.1016/j.phrs.2018.08.013
- [19] Fletcher JA, Rubin BP. KIT mutations in GIST. *Current Opinion in Genetics & Development*. 2007;**17**(1):3-7. DOI:10.1016/j.gde.2006.12.010
- [20] Broekman F, Giovannetti E, Peters GJ. Tyrosine kinase inhibitors: Multi-targeted or single-targeted? *World Journal of Clinical Oncology*. 2011;**2**(2):80-93. DOI: 10.5306/wjco.v2.i2.80
- [21] Bayazeid O, Rahman T. Correlation analysis of target selectivity and side effects of fda-approved kinase inhibitors. *Chemistry Select*. 2021;**6**(30):7799-7814
- [22] Casado P, Alcolea MP, Iorio F, et al. Phosphoproteomics data classify hematological cancer cell lines according to tumor type and sensitivity to kinase inhibitors. *Genome Biology*. 2013;**14**(4):R37. DOI: 10.1186/gb-2013-14-4-r37
- [23] Chakraborty S, Lin YH, Leng X, et al. Activation of Jak2 in patients with blast crisis chronic myelogenous leukemia: Inhibition of Jak2 inactivates Lyn kinase. *Blood Cancer Journal*. 2013;**3**(9):e142. DOI: 10.1038/bcj.2013.41
- [24] Gambacorti-Passerini C, Aroldi A, Cordani N, Piazza R. Chronic myeloid leukemia: Second-line drugs of choice. *American Journal of Hematology*. 2016;**91**(1):67-75. DOI: 10.1002/ajh.24247
- [25] Saglio G, Kim DW, Issaragrisil S, et al. Nilotinib versus imatinib for newly diagnosed chronic myeloid leukemia. *The New England Journal of Medicine*. 2010;**362**(24):2251-2259. DOI: 10.1056/NEJMoa0912614
- [26] Manley PW, Druceckes P, Fendrich G, et al. Extended kinase profile and properties of the protein kinase inhibitor nilotinib. *Biochimica et Biophysica Acta* 2010;**1804**(3):445-453. doi:10.1016/j.bbapap.2009.11.008
- [27] Weisberg E, Manley P, Mestan J, Cowan-Jacob S, Ray A, Griffin JD. AMN107 (nilotinib): A novel and selective inhibitor of BCR-ABL. *British Journal of Cancer*. 2006;**94**(12):1765-1769. DOI: 10.1038/sj.bjc.6603170
- [28] Zhou N, Xu Y, Liu X, et al. Combinatorial pharmacophore-based 3D-QSAR analysis and virtual screening of FGFR1 inhibitors. *International Journal of Molecular Sciences*. 2015;**16**(6):13407-13426. DOI: 10.3390/ijms160613407
- [29] Sharma A, Thelma BK. Pharmacophore modeling and virtual screening in search of novel Bruton's tyrosine kinase inhibitors. *Journal of*

Molecular Modeling. 2019;**25**(7):179.
DOI: 10.1007/s00894-019-4047-y

[30] Srivastava S, Mehta P, Sharma O, Sharma M, Malik R. Computationally guided identification of Akt-3, a serine/threonine kinase inhibitors: Insights from homology modelling, structure-based screening, molecular dynamics and quantum mechanical calculations. *Journal of Biomolecular Structure & Dynamics*. 2020;**38**(14):4179-4188.
DOI: 10.1080/07391102.2019.1675536

[31] Hu Y, Zhou L, Zhu X, Dai D, Bao Y, Qiu Y. Pharmacophore modeling, multiple docking, and molecular dynamics studies on Wee1 kinase inhibitors. *Journal of Biomolecular Structure & Dynamics*. 2019;**37**(10):2703-2715.
DOI: 10.1080/07391102.2018.1495576

[32] Li Y, Pu Y, Liu H, et al. Discovery of novel wee1 inhibitors via structure-based virtual screening and biological evaluation. *Journal of Computer-Aided Molecular Design*. 2018;**32**(9):901-915.
DOI: 10.1007/s10822-018-0122-1

[33] Holderbach S, Adam L, Jayaram B, Wade RC, Mukherjee G. RASPD+: Fast protein-ligand binding free energy prediction using simplified physicochemical features. *Frontiers in Molecular Biosciences*. 2020;**7**:601065.
DOI: 10.3389/fmolb.2020.601065

[34] Wang S, Liu D, Ding M, et al. SE-OnionNet: A convolution neural network for protein-ligand binding affinity prediction. *Frontiers in Genetics*. 2021;**11**:607824. DOI: 10.3389/fgene.2020.607824

[35] Macari G, Toti D, Pasquadibisceglie A, Polticelli F. Docking app RF: A state-of-the-art novel scoring function for molecular docking in a user-friendly Interface to auto

dock Vina. *International Journal of Molecular Sciences*. 2020;**21**(24):9548.
DOI: 10.3390/ijms21249548

[36] Ballester PJ, Mitchell JBA. Machine learning approach to predicting protein-ligand binding affinity with applications to molecular docking. *Bioinformatics*. 2010;**26**(9):1169-1175. DOI: 10.1093/bioinformatics/btq112

[37] Kalinichenko E, Faryna A, Bozhok T, Panibrat A. Synthesis, In vitro and In Silico anticancer activity of new 4-Methylbenzamide derivatives containing 2,6-substituted purines as potential protein kinases inhibitors. *International Journal of Molecular Sciences*. 2021;**22**(23):12738.
DOI: 10.3390/ijms222312738

[38] Kalinichenko E, Faryna A, Kondrateva V, et al. Synthesis, biological activities and docking studies of novel 4-(Arylaminoethyl) benzamide derivatives as potential tyrosine kinase inhibitors. *Molecules*. 2019;**24**(19):3543. DOI: 10.3390/molecules24193543

[39] Wójcikowski M, Ballester PJ, Siedlecki P. Performance of machine-learning scoring functions in structure-based virtual screening. *Scientific Reports*. 2017;**7**:46710. DOI: 10.1038/srep46710

[40] Nagar B, Bornmann WG, Pellicena P, et al. Crystal structures of the kinase domain of c-Abl in complex with the small molecule inhibitors PD173955 and imatinib (STI-571). *Cancer Research*. 2002;**62**(15):4236-4243

[41] Roskoski R Jr. Classification of small molecule protein kinase inhibitors based upon the structures of their drug-enzyme complexes. *Pharmacological Research*. 2016;**103**:26-48. DOI: 10.1016/j.phrs.2015.10.021

- [42] Vijayan R.S, He P, Modi V, et al. Conformational analysis of the DFG-out kinase motif and biochemical profiling of structurally validated type II inhibitors. *Journal of Medicinal Chemistry* 2015;**58**(1):466-479. doi:10.1021/jm501603h
- [43] Wan PT, Garnett MJ, Roe SM, et al. Mechanism of activation of the RAF-ERK signaling pathway by oncogenic mutations of B-RAF. *Cell*. 2004;**116**(6):855-867. DOI: 10.1016/s0092-8674(04)00215-6
- [44] Chan WW, Wise SC, Kaufman MD, et al. Conformational control inhibition of the BCR-ABL1 tyrosine kinase, including the gatekeeper T315I mutant, by the switch-control inhibitor DCC-2036. *Cancer Cell*. 2011;**19**(4):556-568. DOI: 10.1016/j.ccr.2011.03.003
- [45] O'Hare T, Shakespeare WC, Zhu X, et al. AP24534, a pan-BCR-ABL inhibitor for chronic myeloid leukemia, potently inhibits the T315I mutant and overcomes mutation-based resistance. *Cancer Cell*. 2009;**16**(5):401-412. DOI: 10.1016/j.ccr.2009.09.028
- [46] Suebsuwong C, Pinkas DM, Ray SS, et al. Activation loop targeting strategy for design of receptor-interacting protein kinase 2 (RIPK2) inhibitors. *Bioorganic & Medicinal Chemistry Letters*. 2018;**28**(4):577-583. DOI: 10.1016/j.bmcl.2018.01.044
- [47] Adasme MF, Linnemann KL, Bolz SN, et al. PLIP 2021: Expanding the scope of the protein-ligand interaction profiler to DNA and RNA. *Nucleic Acids Research*. 2021;**49**(W1):W530-W534. DOI: 10.1093/nar/gkab294
- [48] NCI Chemical Identifier Resolver. Available from: <http://cactus.nci.nih.gov/chemical/structure> [Accessed: December 13, 2021]
- [49] Trott O, Olson AJ. AutoDock Vina: Improving the speed and accuracy of docking with a new scoring function, efficient optimization, and multithreading. *Journal of Computational Chemistry*. 2010;**31**(2):455-461. DOI: 10.1002/jcc.21334
- [50] Alhossary A, Handoko SD, Mu Y, Kwoh CK. Fast, accurate, and reliable molecular docking with QuickVina 2. *Bioinformatics*. 2015;**31**(13):2214-2216. DOI: 10.1093/bioinformatics/btv082
- [51] Berman HM, Westbrook J, Feng Z, et al. The protein data Bank. *Nucleic Acids Research*. 2000;**28**(1):235-242. DOI: 10.1093/nar/28.1.235
- [52] Slade D. PARP and PARG inhibitors in cancer treatment. *Genes & Development*. 2020;**34**(5-6):360-394. DOI: 10.1101/gad.334516.119
- [53] Abdeldayem A, Raouf YS, Constantinescu SN, Moriggl R, Gunning PT. Advances in covalent kinase inhibitors. *Chemical Society Reviews*. 2020;**49**(9):2617-2687. DOI: 10.1039/c9cs00720b
- [54] Pettersen EF, Goddard TD, Huang CC, et al. UCSF chimera--a visualization system for exploratory research and analysis. *Journal of Computational Chemistry*. 2004;**25**(13):1605-1612. DOI: 10.1002/jcc.20084
- [55] Van Der Spoel D, Lindahl E, Hess B, Groenhof G, Mark AE, Berendsen HJ. GROMACS: Fast, flexible, and free. *Journal of Computational Chemistry*. 2005;**26**(16):1701-1718. DOI: 10.1002/jcc.20291
- [56] Sousa da Silva AW, Vranken WF. ACPYPE - AnteChamber PYthon parser interface. *BMC Research Notes*.

2012;5:367. DOI: 10.1186/1756-0500-5-367

[57] Kollman PA, Massova I, Reyes C, et al. Calculating structures and free energies of complex molecules: Combining molecular mechanics and continuum models. *Accounts of Chemical Research*. 2000;33(12):889-897. DOI: 10.1021/ar000033j

[58] Pu C, Yan G, Shi J, Li R. Assessing the performance of docking scoring function, FEP, MM-GBSA, and QM/MM-GBSA approaches on a series of PLK1 inhibitors. *Medchemcomm*. 2017;8(7):1452-1458. DOI: 10.1039/c7md00184c

[59] Genheden S, Ryde U. The MM/PBSA and MM/GBSA methods to estimate ligand-binding affinities. *Expert Opinion in Drug Discovery*. 2015;10(5):449-461. DOI: 10.1517/17460441.2015.1032936

[60] Kumari R, Kumar R. Open source drug discovery consortium, Lynn a. `g_mmpbsa`--a GROMACS tool for high-throughput MM-PBSA calculations. *Journal of Chemical Information and Modeling*. 2014;54(7):1951-1962. DOI: 10.1021/ci500020m

[61] Valdés-Tresanco MS, Valdés-Tresanco ME, Valiente PA, Moreno E. `gmx_MMPBSA`: A new tool to perform end-state free energy calculations with GROMACS. *Journal of Chemical Theory and Computation*. 2021;17(10):6281-6291. DOI: 10.1021/acs.jctc.1c00645

[62] Li H, Leung KS, Wong MH, Ballester PJ. Improving AutoDock Vina using random Forest: The growing accuracy of binding affinity prediction by the effective exploitation of larger data sets. *Molecular Informatics*. 2015;34(2-3):115-126. DOI: 10.1002/minf.201400132